The Journal of Neuroscience, June 15, 2002, 22(12):5118–5128

How Noise Contributes to Contrast Invariance of Orientation Tuning in Cat Visual Cortex

D. Hansel[1,2] and C. van Vreeswijk[1]

[1]*Laboratoire de Neurophysique et Physiologie du Système Moteur (EP 1848 Centre National de la Recherche Scientifique), Université René Descartes, 75270 Paris cedex 06, France, and* [2]*Center for Neural Computation, Hebrew University, Jerusalem 91904, Israel*

The width of the orientation tuning curves of the spike response of neurons in V1 is invariant to contrast. This property constrains the possible mechanisms underlying orientation selectivity. It has been suggested that noise circumvents the iceberg effect that would prevent contrast invariance in the purely feedforward mechanism. Here we investigate systematically how noise contributes to the contrast invariance of orientation tuning curves in V1. We study three models of increasing complexity: a simple threshold-linear firing rate model, a leaky integrate-and-fire model, and a conductance-based model. We show that the noise transmutes the threshold nonlinearity of the input–output relationships into an approximate power law without a threshold within some firing rate range. This implies that, under certain conditions which are derived here, the tuning of the neuron output is approximately contrast invariant. In particular we show that this mechanism for contrast invariance requires that the neuron firing rate must not be too large and that increasing or lowering the contrast too much destroys this invariance. We also show that if this mechanism operates in V1, the spike response, R, and average voltage response V of the neurons in V1 should vary with the contrast, C, according to $R(C) \propto V(C)^{\gamma}$. The exponent γ can be estimated from the amount by which the spike tuning curve is sharpened with respect to the voltage tuning curves of the neurons. This prediction does not depend on the specifics of the model and can be tested experimentally.

Key words: orientation selectivity; primary visual cortex; V1; contrast invariance; noise; integrate-and-fire model; conductance-based model

The spike response of neurons in V1 is tuned to stimulus orientation (Hubel and Wiesel, 1962). Although the amplitude of the responses increases with the contrast, the width of the tuning curves remains remarkably constant (Sclar and Freeman, 1982; Li and Creutzfeld, 1984; Skottun et al., 1987). This "contrast invariance" is puzzling because of the so-called iceberg effect (Sompolinsky and Shapley, 1997), which predicts that the tuning will be broader at higher contrast as the responses to nonpreferred orientation rise above the spiking threshold. In the past 15 years, several mechanisms have been proposed to avoid this effect (Ben-Yshai et al., 1995, 1997; Somers et al., 1995; Hansel and Sompolinsky, 1998; Troyer et al., 1998; Ferster and Miller, 2000).

Recently it has been shown that the tuning curves of the membrane potential of neurons in V1 are also contrast invariant with a mean response subthreshold and substantial fluctuations (Anderson et al., 2000a). Other experimental groups (Arieli et al., 1996; Tsodyks et al., 1999) have pointed out the crucial effect of noise on voltage in the firing of neurons in V1.

Using numerical simulations, Anderson et al. (2000a) showed for a rate model that this noise can effectively "smooth" the threshold nonlinearity. This, combined with the contrast invariance of the average membrane potential tuning, leads to contrast-invariant spike-response tuning curves.

These observations raise several questions. (1) The noise smoothes the iceberg effect in precisely such a way that the output of the neuron is contrast invariant. How can this seemingly miraculous effect be explained? (2) Anderson et al. (2000a) used a rate model with a threshold linear transfer function. How important is it for the transfer function to have this form? (3) This paper reports results from cells that have a low firing rate with a maximum of 8 Hz for simple cells, whereas complex cells have rates below 40 Hz. These firing rates are much lower than those reported elsewhere (Sclar and Freeman, 1982; Skottun et al., 1987; Anderson et al., 2000b). Can the proposed mechanism still hold for cells that fire more vigorously? (4) Intracellular recordings show that voltage fluctuations are on a time scale that is similar to many of the processes that make up the internal dynamics of the neuron (Borg-Graham et al., 1998; Anderson et al., 2000a). With such rapid fluctuations in the voltage, to what extent do the results from a rate description of the neuronal dynamics correspond to the actual behavior of the neurons in V1 (Ermentrout, 1994; Shriki et al., 1998; Gerstner, 2000; Brunel et al., 2001)? How does the proposed mechanism apply when the kinetics of active channels are taken into account? Here we investigate all these questions theoretically, using three models of neurons of increasing complexity and biophysical realism.

MATERIALS AND METHODS

In this paper we consider neurons in V1 stimulated with drifting gratings. We focus on the role of noise in contrast invariance of the tuning for complex cells. Our analysis is simplified in that case because according to

Received Jan. 29, 2002; revised March 12, 2002; accepted March 15, 2002.

This research was supported in part by the PICS-CNRS 867 and by the National Science Foundation under Grant PHY99-07949. We thank R. Shapley and H. Sompolinsky for fruitful discussions and Y. Yarom for careful reading of this manuscript.

Correspondence should be addressed to Dr. David Hansel, Laboratoire de Neurophysique et Physiologie du Système Moteur, 45 Rue des Saints-Pres 75270 Paris, France. E-mail: david.hansel@biomedicale.univ-paris5.fr.

 0270-6474/02/225118-11$15.00/0

the classical view we can assume that the inputs to the cells are not temporally modulated.

Rate models. In a rate model the firing rate, R, is a nonlinear function of the voltage, V, $R = g(V)$. The voltage, V, consists of an average part $\bar{V}$, which is a deterministic function of the input and a noise that varies from trial to trial. Following the experimental results of Anderson et al. (2000a), we assume that the tuning of the mean voltage response to the input is contrast invariant. We also include a contribution, V_0, to the mean contrast, $\bar{V}$, that does not depend on the input:

$$\bar{V}(C, \theta) = V_0 + V_m(C)\kappa_V(\theta), \quad (1)$$

where V_m is the voltage response at the preferred orientation, $\theta = \theta_0$, and κ_V is the normalized tuning curve for the mean voltage, with $\kappa_V(\theta_0) = 1$. Without loss of generality we can assume that $\theta_0 = 0$. Consistent with experimental results we will also assume that κ_V is symmetric around $\theta = 0$ and that the voltage tuning curve is unimodal.

The Anderson et al. (2000a) experiments show that in V1 the amplitude of the noise is not or only weakly dependent on the contrast and orientation of the input. We will therefore assume input-independent noise. The noise can be written as $\sigma\eta$, where σ is the SD, and η is a random variable drawn from some distribution with mean 0 and SD 1. Given this distribution, we can write for the average spike rate, $\bar{R}$, for an input with contrast C and orientation θ:

$$\bar{R}(C, \theta) = \langle g(\bar{V}(C, \theta) + \sigma\eta)\rangle_\eta \equiv G_\sigma(\bar{V}(C, \theta)). \quad (2)$$

Here we have used $\langle\cdot\rangle_\eta$ to denote averaging over the noise. Note that even if the neuronal dynamics is complex and not given by a simple rate equation, the average firing rate is still given by the equation $\bar{R}(C, \theta) = G_\sigma(\bar{V}(C, \theta))$, after averaging over the input-independent noise, provided that the input to the neuron varies sufficiently slowly. The function G_σ, however, may not be easy to evaluate in this case.

We first derive conditions that G_σ must satisfy to ensure that the rate tuning is contrast invariant. Then we assume that the transfer function g is a threshold linear function, $g(V) = \beta[V - V_T]_+$, where V_T is a threshold and β the gain. The half-rectifying function is denoted by $[x]_+$, $[x]_+ = 0$ for $x < 0$ and $[x]_+ = x$ for $x \geq 0$. For a Gaussian noise, the noise-averaged transfer function, G_σ, can be determined analytically. This function does not satisfy the requirements for contrast invariance of the spike rate exactly, but the region of approximated compliance to the requirement is determined using standard mathematical techniques.

The integrate-and-fire model. We model a complex cell as a leaky integrate-and-fire neuron (Lapicque, 1907). The neuron receives a stimulus-dependent input current, $I(C, \theta) = I_m(C)\kappa_I(\theta)$, as well as a stimulus-independent input I_0 and stimulus-independent Gaussian noise, $\sigma\eta$. The input tuning κ_I is a Gaussian with a half-width at half-maximal of 30°. Subthreshold, the voltage, V, of the cell satisfies:

$$C_M\frac{dV}{dt} = g_L(V_{rest} - V) + I_0 + I(C, \theta) + \sigma\eta(t). \quad (3)$$

Here, C_M is the membrane capacitance, g_L the leak conductance, and V_{rest} the resting potential. As the voltage reaches the threshold, V_T, a spike occurs and V is immediately reset to a potential V_{reset}. The average firing rate $\bar{R}$, the mean membrane potential $\bar{V}$, and the SDs of the voltage fluctuations, σ_V, are calculated analytically as functions of the input current I. The conditions under which contrast-invariant input tuning leads to approximate contrast-invariant mean firing rate and average voltage tuning are determined numerically.

Conductance-based neurons. The mono-compartmental conductance-based model we consider describes a regular spiking (excitatory) cell in V1. It has the form:

$$C_M\frac{dV}{dt} = I(C, \theta) + I_L + I_{Na} + I_{NaP} + I_K + I_A + I_{Ks}, \quad (4)$$

where V is the membrane potential of the neuron and C_M its membrane capacitance. We take $C_M = 1$ nF/cm^2. The first term in the right-hand side of this equation is the external input. The second term is the leak current $I_L = g_L(V_L - V)$, with $g_L = 0.2$ mS/cm^2 and $V_L = -70$ mV. Note that with this value of leak conductance, the passive time constant of the cell is 5 msec, which is larger than what is usually considered as typical for regular spiking cells. However, when embedded into cortical networks, the input conductance of neurons increases substantially (Bernander et al., 1991; Rapp et al., 1992) because of synaptic interactions with other cells in the network. This network is not modeled here. That is why we have assumed a larger leak conductance to take these interactions into account.

Table 1. Gating variables of the conductance-based model: $x_\infty = [a_x/(a_x + b_x)]$, $\tau_x = [1/(a_x + b_x)]$ for $x = m, h, n$; τ_x is in milliseconds

x	a_x	b_x
m	$\frac{0.1(V+35)}{1-\exp(-0.1(V+35))}$	$4\exp(-(V+60)/18)$
h	$0.35\exp(-(V+58)/20)$	$\frac{5}{\exp(-0.1(V+28))+1}$
n	$\frac{0.05(V+34)}{1-\exp(-0.1(V+34))}$	$0.625\exp(-(V+44)/80)$
x	x_∞	τ_x
a	$\frac{1}{1+\exp(-(V+50)/20)}$	Instantaneous
b	$\frac{1}{1+\exp((V+80)/6)}$	20
s	$\frac{1}{1+\exp(-(v+40)/5)}$	Instantaneous
z	$\frac{1}{1+\exp(-0.7(V+30))}$	50

Table 2. Conductance density in microSiemens per centimeters squared and reversal potentials in millivolts for the ionic channels in the conductance-based model

x	g_x	V_x
Na	35	55
NaP	0.08	55
K	15	−90
A	2.5	−90
K_s	0.5	−90

The model incorporates five ionic currents: a sodium Hodgkin–Huxley-like current: $I_{Na} = -g_{Na}m_\infty^3 h(V - V_{Na})$; a persistent sodium current: $I_{NaP} = -g_{NaP}s_\infty(V)(V - V_{Na})$; a delayed rectifier potassium current: $I_K = -g_K n^4(V - V_K)$; an A-type potassium current: $I_A = -g_A a_\infty(V)^3 b(V - V_K)$; and a slow potassium current, K_s, responsible for spike adaptation: $I_{Ks} = -g_{Ks}z(V - V_K)$.

The dynamical equations for the gating variables are:

$$\frac{dx}{dt} = \frac{x_\infty(V) - x}{\tau_x(V)}, \quad (5)$$

where $x = h, n, b, z$. All the functions $x_\infty(V)$, τ_x and the other gating variables are given in Table 1. The respective maximum conductance densities and the reversal potentials of the ionic currents are given in Table 2.

For the external current we assume that a complex cell receives its input from N simple cells, which are tuned for orientation. These simple cells fire spikes according to Poisson processes that are uncorrelated across the cells. Therefore we model the external current as:

$$I(C, \theta, t) = g(C, \theta, t)(V_{syn} - V), \quad (6)$$

where the reversal potential $V_{syn} = 0$ mV, and g is a conductance change that depends on the contrast and stimulus orientation. It represents the pooled contribution of all the conductance changes induced by the synapses from all the input simple cells. It is modeled as:

$$g(C, \theta, t) = \bar{g}\sum_i f(t - t_i), \quad (7)$$

where $\bar{g}$ characterizes the strength of the synapses impinging on the cell and:

$$f(t) = \frac{1}{\tau_1 - \tau_2}[\exp(-t/\tau_2) - \exp(-t/\tau_1)]\Theta(t), \quad (8)$$

with $\Theta(t) = 1$ if $t > 0$ and $\Theta(t) = 0$ otherwise, and t_i is a sequence of random events with Poisson statistics. The rate of the Poisson process is:

$$\rho(C, \theta) = \rho_0 + \rho_1(C)\exp(-\theta^2/2\Delta^2). \quad (9)$$

The first term is untuned. It describes the spontaneous activity of the simple cells. The second term corresponds to the effect of the visual stimulus. The parameter Δ characterizes the degree of tuning of this effect. The dependence of $\rho_1(C)$ on the contrast will not be modeled here in detail. We simply assume that it is an increasing function of the contrast, and we study the effect of changing the contrast by increasing ρ_1. The parameter values used in our simulations are $\tau_1 = 1$ msec, $\tau_2 = 3$ msec, $\bar{g} = 0.5$ mS/cm^2, $V_{syn} = 0$ mV.

As for the integrate-and-fire model described above, a Gaussian stimulus-independent white noise, $\sigma\eta(t)$, is added to the external current. This noise describes the fluctuating part of the network feedback into the neuron.

The dynamical equations were integrated numerically using a fourth-order Runge–Kutta scheme with a fixed time step ($dt = 0.025$ msec). The tuning curves of the output firing rate of the neuron were fitted with a Gaussian, $R = A_r \exp(-\theta^2/2\Delta_r^2)$. The tuning curves of the average potential were computed without clipping of the spikes and were fitted with a Gaussian $\bar{V} = A_v \exp(-\theta^2/2\Delta_v^2) + C_v$. The tuning curves of the membrane potential fluctuations were computed after cutting the spikes, taking the depolarization of the neuron at the rheobase as a threshold value.

RESULTS

Conditions for contrast invariance for a general rate model

In general the noise-averaged transfer function G_σ (Eq. 2) does not transform a contrast invariant voltage into a contrast invariant average rate $\bar{R}(C, \theta)$. What constraints does G_σ have to satisfy to insure this?

Assuming no stimulus independent contribution, $V_0 = 0$, contrast invariance of the spike and voltage tuning implies that:

$$R_m(C)\kappa_R(\theta) = G_\sigma(V_m(C)\kappa_V(\theta)), \quad (10)$$

where R_m is the average rate at the preferred orientation, and κ_R the normalized spike tuning curve, with $\kappa_R(0) = 1$.

Taking the derivative with respect to C and θ, respectively, yields:

$$R_m'(C)\kappa_R(\theta) = G_\sigma'(V)V_m'(C)\kappa_V(\theta) \quad (11)$$

$$R_m(C)\kappa_R'(\theta) = G_\sigma'(V)V_m(C)\kappa_V'(\theta), \quad (12)$$

where the prime indicates the derivative. These equations have two solutions:

$$G_\sigma'(V) = 0 \text{ or } \frac{\frac{d}{dC}\log(|R_m(C)|)}{\frac{d}{dC}\log(|V_m(C)|)} = \frac{\frac{d}{d\theta}\log(|\kappa_R(\theta)|)}{\frac{d}{d\theta}\log(|\kappa_V(\theta)|)} = \alpha, \quad (13)$$

where α is a constant. The first solution, $G_\sigma'(V) = 0$, leads to $\bar{R} = R_0$. The second solution implies $\log(|\bar{R}|) = \alpha \log(|\bar{V}|) + \log(A)$, where A is a positive constant. Thus in this solution $\bar{R}$ is given by $\bar{R} = A|\bar{V}|^\alpha$. Because G_σ gives the average firing rate after the noise is taken into account, it should be a continuous function. Making the plausible assumptions that the rate is a nondecreasing function of the mean voltage, and that it goes to zero for $\bar{V} \to -\infty$, G_σ must have the form:

$$G_\sigma(V) = \begin{cases} 0 & \text{for } V \lambda_e 0 \\ AV^\alpha & \text{for } V > 0 \end{cases} \quad (14)$$

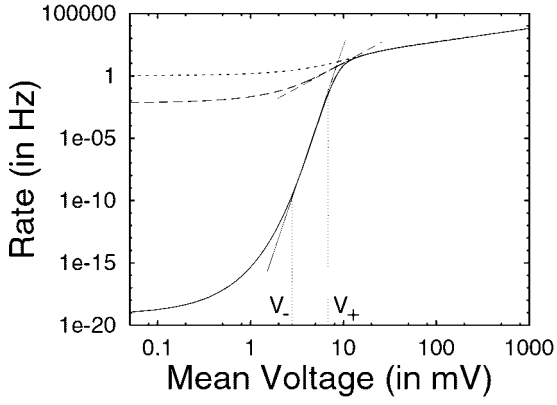

Figure 1. For voltage fluctuations of the right size the firing rate of the neuron is well approximated by a power of the input over the physiological range. The figure shows a log–log plot of firing rate as a function of voltage for different levels of noise, $\sigma = 1$ mV (*dotted line*), $\sigma = 3$ mV (*dashed line*), and $\sigma = 6$ mV (*solid line*). To highlight the qualitative features of the neuronal response, the rate is plotted well outside the range that can be measured in experiments. For $\sigma = 1$ mV and $\sigma = 3$ mV, the power law approximation is also shown (*thin dashed* and *solid line*, respectively). For $\sigma = 1$ mV the power law behavior only extends rates up to 10^{-3} Hz. For $\sigma = 3$ mV the power law behavior is observed between 0.1 and 30 Hz, whereas for larger noise ($\sigma = 6$ mV) the rate is non-negligible even at the resting voltage. Other parameters: $\beta = 6$ Hz/mV, $V_T = 9$ mV, $V_0 = 0$ mV.

where α and A are positive. Therefore:

$$R_m(C) = AV_m(C)^\alpha \quad (15)$$

$$\kappa_R(\theta) = \kappa_V(\theta)^\alpha. \quad (16)$$

This implies that $\kappa_V(\theta_{HWHM}) = 1/2^{1/\alpha}$, where θ_{HWHM} is the half-width at half-maximal of the spike response (defined by $\kappa_R(\theta_{HWHM}) = 1/2$). Therefore, the larger the α, the sharper the tuning of the spike response.

Approximate contrast invariance for a threshold-linear transfer function

Let us assume a threshold-linear transfer function, $g(V) = \beta[V - V_T]_+$ and a Gaussian noise. In Appendix A it is shown that G_σ is given by:

$$G_\sigma(\bar{V}) = \beta\sigma\left\{\frac{\bar{V} - V_T}{\sigma}H\left(-\frac{\bar{V} - V_T}{\sigma}\right) + \frac{1}{\sqrt{2\pi}}\exp\left(-\frac{(\bar{V} - V_T)^2}{2\sigma^2}\right)\right\}, \quad (17)$$

where $H(x) = (2\pi)^{-1/2}\int_x^\infty e^{-y^2/2}\,dy$ is the complementary error function.

Clearly $G_\sigma(\bar{V}) \neq A[\bar{V}]_+^\alpha$ for any value of σ. Therefore, according to the analysis in the previous paragraph, exact contrast invariance is not expected to occur. However, as we show now, some range of the noise level, σ, $G_\sigma(\bar{V})$ is well approximated by a power law for a large range of $\bar{V}$.

Figure 1 displays a log–log plot of the function G_σ against $\bar{V}$, for different values of σ. For all the values of σ, for large enough $\bar{V}$, the curves overlap and are linear, satisfying $\log(G_\sigma) = \log(\bar{V}) + \log(\beta)$. This is because for high voltages the effect of the threshold nonlinearity becomes negligible. For small values of $\bar{V}$, the curves approach a finite limit, which for $\sigma \ll V_T$ is exponentially small. To smoothly connect these two regions the curves need to begin to rise with a slope that increases with $\log(\bar{V})$. At some point, $\bar{V} = V^*$, the slopes reach a maximum larger than 1

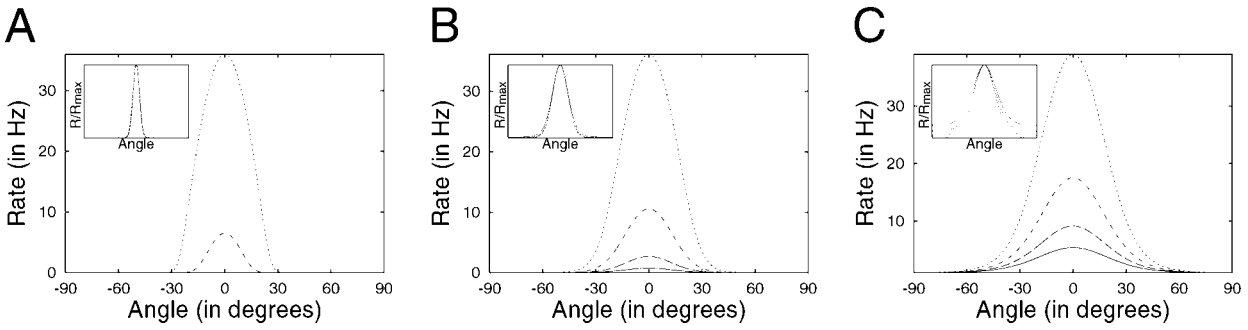

Figure 2. Power law behavior of the voltage-rate relation causes the rate tuning to be contrast invariant. The rate tuning curves are shown for different levels of noise: *A*, $\sigma = 1$ mV; *B*, $\sigma = 3$ mV; *C*, $\sigma = 6$ mV. Each panel shows the rate response to a Gaussian mean voltage, with half-width at half-maximal of 30°, with different maximum voltage: 5 mV (*solid line*), 7 mV (*long dashed line*), 10 mV (*short dashed line*), and 15 mV (*dotted line*). The *insets* show the corresponding normalized rate tuning curves. Note that in A the response to 5 and 7 mV is so small as to be indistinguishable from 0 Hz. Other parameters are as in Figure 1. Only for a voltage noise $\sigma = 3$ mV are the tuning curves for the firing rate contrast invariant. For $\sigma = 1$ mV, the firing rate exceeds the region in which the power law holds, causing broadening of the tuning curve for larger contrast. For large voltage fluctuations, $\sigma = 6$ mV, the rate does not go to 0 Hz at the null orientation, resulting in contrast dependence at the null orientation for the normalized tuning curves.

and start to decrease, i.e., they display an inflection point. Because at this inflection point ($\bar{V} = V^*$) the second derivative of the curve is zero, there is a region around $\log(V^*)$, from $\log(V^-)$ to $\log(V^+)$, at which the curve is well approximated by $\log(G) = \alpha \log(V) + \log(A)$, as indicated in Figure 1. This figure also shows that the slope α increases as σ is decreased.

If σ is sufficiently small, V^- is exponentially small, and below V^- the rate is negligible. By construction $G_\sigma(\bar{V}) \approx A\bar{V}^\alpha$ for $V^- < \bar{V} < V^+$, and hence, for all $\bar{V} < V^+$, G_σ can indeed be approximated by $G_\sigma(\bar{V}) = A[\bar{V}]_+^\alpha$, provided that σ is not too large. On the other hand, if σ is too small, V^+ is relatively small, and $G_\sigma(V^+)$ becomes extremely small. Therefore to achieve both sharp tuning of the spike response and invariance of this tuning over a substantial range of contrasts, an intermediate noise level must be selected.

This is demonstrated in Figure 2: *A, B,* and *C* show the spike tuning of a cell for $\sigma = 1$ mV, 3 mV, and 6 mV, respectively. In each panel the spike response for a mean voltage $\bar{V} = V_m \exp(-\theta^2/2\Delta^2)$ with different values of V_m is shown. The width Δ is chosen so that the half-width at half-maximal for the voltage is 30°. With $\sigma = 1$ mV (Fig. 2*A*), the maximum firing rate is outside the region in which G_σ can be approximated by a power law. As a result the spike tuning curves are not contrast invariant. This is further demonstrated in the *inset*, which shows the normalized tuning curves. For $\sigma = 3$ mV (Fig. 2*B*), the maximum firing rate stays within the region in which G_σ is closely approximated by a power law with $\alpha = 3.85$, and the normalized spike tuning curves very nearly overlap (*inset*). If σ is increased to 6 mV (Fig. 2*C*), the firing rate at the orthogonal orientation, where the mean voltage is not elevated, is no longer negligible. As a result, the normalized tuning curves do not overlap (*inset*).

Figure 3 shows the half-width at half-maximal for the firing rate for different values of V_m, as a function of the noise level, σ. It demonstrates that approximate contrast invariance can be achieved only if the noise level is $\sigma \approx 2$–4 mV. Beyond this value the width of the spike tuning curve increases rapidly. This is because for sufficiently large values of σ, the baseline rate is of the same order as the maximum elevation of the rate caused by the preferred stimulus.

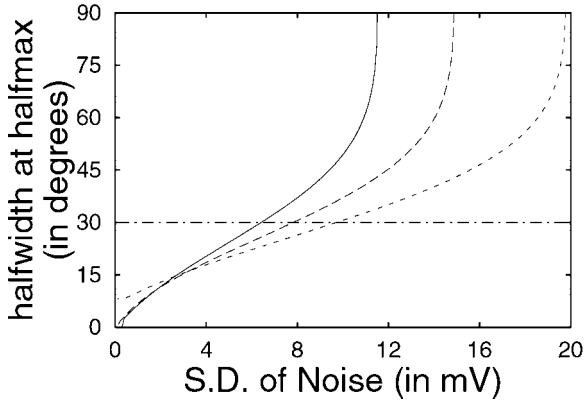

Figure 3. Half-width at half-maximal of the rate response as function of the noise level for different values of the maximum voltage response: $V_{max} = 5$ mV (*solid line*), $V_{max} = 10$ mV (*dashed line*), $V_{max} = 15$ mV (*dotted line*). Other parameters as in Figure 1. For small voltage fluctuations the tuning is much more sharpened, but different for contrasts, whereas for very high levels of noise the rate at the null orientation is more than half the rate at the preferred orientation, resulting in a divergence of the half-width at half-maximal. Only for a noise with a SD of ~3 mV is the half-width at half-maximal the same for all contrasts, reflecting the contrast invariance for this noise level.

The effect of a stimulus-independent input

So far we have assumed that there is no stimulus-independent mean voltage, $V_0 = 0$. We will now discuss the effect of adding a non-zero stimulus-independent voltage. The firing rate of the neuron is a function of $(\bar{V} - V_T)/\sigma$:

$$R = r\left(\frac{\bar{V} - V_T}{\sigma}\right), \tag{18}$$

where r is given by Equation 17. Because it is the stimulus-dependent part of the average voltage that is contrast invariant, we would like to describe the rate as a function of the mean voltage response, V_{resp}, which is given by $V_{resp} = \bar{V} - V_0$. The firing rate can be written as:

$$R = r\left(\frac{V_{resp} - V_{T,ef}}{\sigma}\right), \tag{19}$$

where the effective threshold, $V_{T,eff}$, satisfies $V_{T,eff} = V_T - V_0$. This demonstrates that including a positive stimulus-independent part in the input has the effect of reducing the threshold. Alternatively, keeping the threshold the same, the rate can be written as:

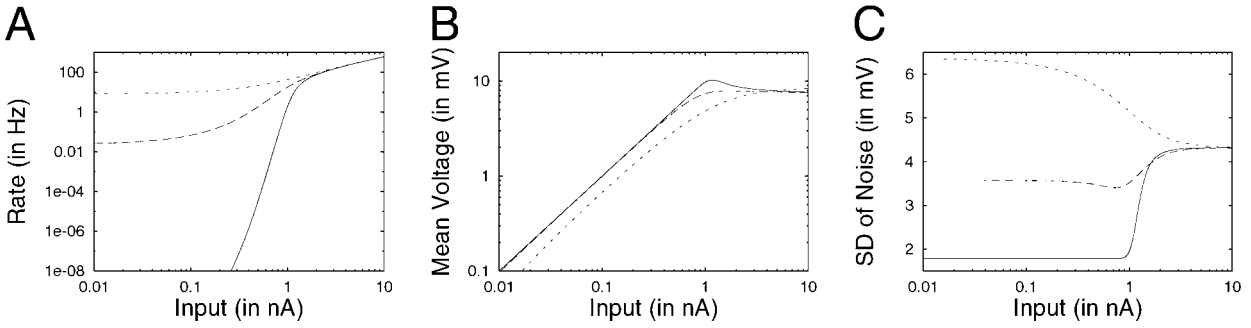

Figure 4. Response of integrate-and-fire neuron for different levels of noise. *A*, Log of firing rate against log mean input current. There is only an approximate power law relation between rate and input current in the range from 1 to 30 Hz, for intermediate values of the input noise. *B*, Log of mean voltage against log mean input current. For all noise levels, the voltage varies linearly with the input up to an input value at which the firing rate becomes appreciable (~5 Hz). *C*, SD of the voltage against log mean input current. For small inputs the SD of the voltage is constant and equal to that of a passive integrator without a spiking mechanism. For very large inputs the voltage fluctuations are dominated by reset of the voltage and the drift back to the threshold, and hence become independent of the noise level of the input. The input current is in microamperes per square centimeters. Parameters: $\sigma = 0.8\ \mu A/cm^2\ (msec)^{1/2}$ (*solid line*), $\sigma = 1.6\ \mu A/cm^2\ (msec)^{1/2}$ (*dashed line*), $\sigma = 3.2\ \mu A/cm^2\ (msec)^{1/2}$ (*dotted line*). Other parameters: $C_M = 1.0\ \mu F/cm^2$, $g_L = 0.1\ mS/cm^2$, $V_{rest} = 0$ mV, $V_T = 15$ mV, and $I_0 = 0$.

$$R = r\left(\frac{V_{resp,ef} - V_T}{\sigma_{ef}}\right), \tag{20}$$

where $\sigma_{eff} = \frac{V_T}{V_T - V_0}\sigma$ and $V_{resp,eff} = \frac{V_T}{V_T - V_0}V_{resp}$. Thus adding a positive stimulus-independent part to the voltage has the effect of either reducing the threshold or alternatively increasing the voltage response and noise level by a factor >1.

Therefore a positive V_0 shifts the interval of the rates over which the power-law relationship between firing rate and voltage holds to higher rates, but decreases the power, thereby reducing the degree of sharpening of the rate response relative to the voltage response.

Contrast invariance in the integrate-and-fire model

For the integrate-and-fire neuron the stochastic Equation 3 leads, after averaging over the noise, to a probability distribution of the voltage. From this distribution the average firing rate, the mean voltage, and SD of the subthreshold voltage fluctuations can be computed (Gluss, 1967; Tuckwell, 1984). These calculations are shown in Appendix B. Here we only give the results.

The mean firing rate $\bar{R}$ is given by:

$$\bar{R} = \frac{1}{\tau_M}\left[\sqrt{2\pi}\int_{x_-}^{x_+} e^{x^2/2}H(x)dx\right]^{-1}, \tag{21}$$

where $\tau_M \equiv C_M/g_L$ is the membrane time constant, and x_- and x_+ are given by $x_- = (\sqrt{2g_L C_M}/\sigma)(V_0 - V_T)$ and $x_+ = (\sqrt{2g_L C_M}/\sigma)(V_0 - V_{reset})$, respectively.

This equation is not readily interpreted and has to be computed numerically. Figure 4*A* shows a log–log plot of the spike rate, $\bar{R}$, versus the input current, I. These curves can be understood qualitatively as follows. For large input currents the firing rate of a noiseless integrate-and-fire neuron increases linearly with the input. This remains true when noise is added. With an average input of $I \approx 0$, the rate is exponentially small for a low noise level. Intermediate values of the input should smoothly interpolate between these regimes. This is analogous to the way the average rate depends on the average voltage in the rate model. Thus the log–log plot of $\bar{R}$ versus I in the integrate-and-fire model is qualitatively similar to that of $\bar{R}$ versus $\bar{V}$ in the rate model. For $\log(I) \to -\infty$, the curves are flat, and for large I the curves merge to a straight line with slope 1. At an intermediate level there is an inflection point, around which the rate varies approximately as a power law of the input, with a higher power for smaller σ. In the figure, $\alpha = 16.5$, for $\sigma = 0.8\ \mu A/cm^2\ (msec)^{1/2}$, $\alpha = 3.25$, for $\sigma = 1.6\ \mu A/cm^2\ (msec)^{1/2}$, and $\alpha = 1.21$, for $\sigma = 3.2\ \mu A/cm^2\ (msec)^{1/2}\ (msec)^{1/2}$ in this intermediate region.

Appendix B also shows that the average voltage is given by:

$$\bar{V} = V_{rest} + g_L^{-1}I - (V_T - V_{reset})\tau_M\bar{R}. \tag{22}$$

Likewise the SD, σ_V, of the voltage can be computed directly (Appendix B). It satisfies:

$$\sigma_V^2 = \frac{\tau_M}{2}\left(\frac{\sigma}{C}\right)^2 + (V_T - V_{reset})\left(\bar{V} - \frac{V_T + V_{reset}}{2}\right)\tau_M\bar{R}. \tag{23}$$

Equation 22 for the average voltage, $\bar{V}$, can be understood straightforwardly. If the firing rate is very small, the effect of the threshold can be ignored. Thus the neuron acts as a passive integrator in this scheme. As a result, the average voltage increases linearly with the input, as long as the spike rate $\bar{R}$ is small. When the firing rate becomes appreciable, this is no longer the case, and the reset current at the time of the spike has to be incorporated. The net effect of a spike is a reset of the voltage from V_T to V_{reset}. In other words, each spike event delivers a net charge of $(V_{reset} - V_T)C_M$ per unit membrane area. Thus the total current into the cell (external plus spike currents) is equal to $I_0 - (V_T - V_{reset})C_M\bar{R}$, resulting in Equation 22 for the average voltage.

When $\bar{R}$ is negligible, the deviation of the average voltage, $\bar{V}$, from the rest potential, V_{rest}, is proportional to the input current, I. Thus the tuning of the average voltage relative to rest is contrast invariant when the input tuning is contrast invariant. If $I(C, \theta) = I_m(C)\kappa_I(\theta)$, $\bar{V}(C, \theta) - V_{rest} = V_m(C)\kappa_V(\theta)$, with, $V_m = I_m/g_L$, and $\kappa_V = \kappa_I$. If the average firing rate becomes too large, $(V_T - V_{reset})\tau_m\bar{R} \approx I/g_L$, and the tuning of the average voltage is no longer contrast invariant.

Figure 4*B* shows a log–log plot of the mean voltage, $\bar{V} - V_{rest}$, against the input current, I, for different noise levels. As expected the mean voltage varies linearly for low input. As I approaches the threshold current, the rate becomes significant, and the voltage increases sublinearly. Somewhat later the rate increase with

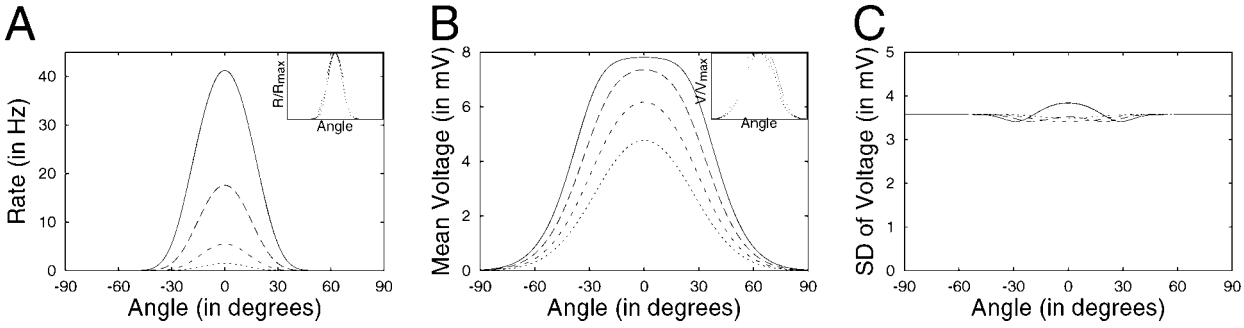

Figure 5. Contrast invariance of the spike rate and voltage tuning of the integrate-and-fire neuron with intermediate input noise. Tuning curves are shown for the integrate-and-fire neuron for different maximum mean input levels I_{max}. *A*, The rate response. *B*, Mean voltage. *C*, SD of voltage fluctuations. The tuning of spike rate is contrast invariant for the whole range of inputs (*inset*), because over the whole range of input the power law relation between input and firing rate holds. Compare Figure 4*A*. For the voltage the contrast independence breaks down for the highest contrast (*inset*). This is because at high contrasts the firing rate at the preferred orientation is large, so that the resetting of the voltage can no longer be neglected. The tuning of the voltage fluctuations is very weak, even for high contrast, because for this input noise level, the SDs of the voltage only weakly depend on the mean input, as seen in Figure 4*C*, *middle curve.* In all graphs: $I_{max} = 5\ \mu A/cm^2$ (*dotted line*), $I_{max} = 7\ \mu A/cm^2$ (*short dashed line*), $I_{max} = 10\ \mu A/cm^2$ (*long dashed line*), and $I_{max} = 15\ \mu A/cm^2$ (*solid line*). Mean input current has Gaussian tuning with half-width at half-maximal of 30°. Parameters: $\sigma = 1.6\ \mu A/cm^2\ (msec)^{1/2}$. Others are as in Figure 4.

input becomes so large that the average voltage decreases with increased input current. It approaches asymptotically $(V_T + V_{reset})/2$. The value of the input current at which the dependence of $\bar{V}$ on I starts to deviate from linear varies with the noise level. The higher σ, the sooner this deviation sets in.

Figure 4*C* shows the SD of the membrane potential, σ_V, computed from Equation 23 as a function of the input. One sees that σ_V is approximately constant for inputs that are not too large. This can be understood as follows. For weak inputs, the effects of the threshold can be ignored, and the neuron integrates the Gaussian noisy input passively. Therefore the equilibrium distribution of the voltage is Gaussian, with a width that does not vary with the mean input. This is reflected in Equation 23: for a firing rate, $\bar{R}$, which is sufficiently small. The second term in Equation 23 is negligible compared with the first one, and therefore $\sigma_V^2 = \tau_M/2(\sigma/C_M)^2$. When the input becomes large, the fluctuations change rapidly because the second term in Equation 23 is no longer negligible. This reflects the fact that for large $\bar{R}$ the resetting caused by the spike is appreciable, and the voltage distribution eventually becomes uniform between V_{reset} and V_T. Depending on the noise level, this high rate distribution may be either broader or narrower than the distribution at low rates, as can be seen from Figure 4*C*.

Comparing Figure 4, *A* and *B*, one sees that the deviation from linearity for the voltage occurs before the deviation from a power law for the rate. Thus with contrast-invariant input tuning, the contrast invariance of the average voltage tuning should break down for contrasts lower than the contrast invariance of the spike tuning. This is confirmed in Figure 5. In Figure 5, *A* and *B*, the tuning curves of $\bar{V}$ and $\bar{R}$, respectively, are shown for different contrasts, with no contrast-invariant current, $I_0 = 0$. For low contrasts the voltage tuning is approximately contrast invariant, but significant deviations occur for high contrast. For the spike rate, however, the tuning is approximately contrast invariant for all levels of contrast shown here. Figure 5*C* shows the tuning curves of σ_V for the same contrasts. It demonstrates that except for the largest contrast the fluctuations of the membrane potential are independent of the stimulus angle. Only for the largest contrast a slight increase of σ_V occurs around the preferred orientation of the neuron. This is because away from the preferred orientation the input current is small, and therefore the SD of the voltage fluctuations is independent of the input, as shown in Figure 4*C*. Only sufficiently close to the preferred orientation is the input current large enough to substantially affect voltage noise level.

The effect of adding a stimulus independent input current, I_0, is similar to adding a stimulus independent voltage V_0 in the rate model. It effectively changes the rest voltage V_{rest} to $V_{rest,eff}$ given by $V_{rest,eff} = V_{rest} + I_0/g_L$ or, alternatively, by changing the threshold voltage V_T and reset V_{reset} to $V_{T,eff} = V_T - I_0/g_L$ and $V_{reset,eff} = V_{reset} - I_0/g_L$. In the region where a power law relation between the firing rate and average voltage exist, the firing rate, mean voltage, and voltage fluctuations are hardly affected by changing the reset voltage. This is because in this region the firing rate is small, and hence the voltage of the neuron is hardly ever reset. Thus adding a stimulus-independent current I_0 has the same effect as changing the threshold voltage from V_T to $V_T - I_0/g_L$. This leads to changes in the neuronal response that are the same as those described for the rate model.

Contrast invariance in the conductance-based model

The conductance-based model was studied numerically. The resting potential of the neuron is $V_{rest} = -70.6$ mV. Onset to periodic firing corresponds to a depolarized membrane potential of $V_c = -57.6$ mV.

Figure 6*A* shows, in a log–log plot, the spike response of the neuron against the average firing rate of the input, ρ, for three different values of noise, σ. One sees that in a range of the input that depends on σ, $\log R$ is linearly related to $\log \rho$ with a slope that decreases with increasing σ. This behavior is similar to what we have found for the integrate-and-fire, with ρ playing the role of the input current I in that model. Figure 6*B* shows $\log R$ as a function of $\log(\rho - \rho_0)$ for $\sigma = 2\ \mu A/cm^2/msec^{1/2}$ and three different values of ρ_0. Here again the dependency is linear with a slope that depends on ρ_0. The range of firing rates over which the approximation is valid also depends strongly on this parameter, as in the rate and integrate-and-fire models.

We now consider the response of the neuron to a visual input modeled according to Equation 9 with half-width at half-maximal of the stimulus-dependent input of 26.5° ($\Delta = 22.5°$), and $\rho_0 = 1500$ Hz. This input induces a change in the input conductance of the neuron, the tuning curve of which is plotted in Figure 7 for

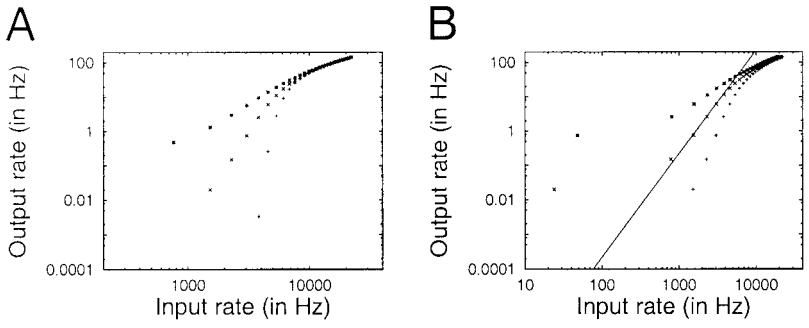

Figure 6. The results obtained for the integrate-and-fire can be extended to conductance-based models. The role of the external input, I, is now played by the input rate ρ. *A*, The logarithm of the output spike rate, $\log R$, against the logarithm of the input rate. In a certain range of the input, $\log R$ and $\log \rho$ are proportional. The input range depends on the SD of the noise, σ, and the proportionality constant decreases with increasing σ as seen by comparing three different noise values. $\sigma = 1$ (*pluses*), $\sigma = 2$ (*crosses*), and $\sigma = 3$ (*stars*). *B*, $\log R$ and $\log(\rho - \rho_0)$ are also proportional in a certain range of input that depends on ρ_0. This is shown by plotting R and $\rho - \rho_0$ in log–log scale for $\sigma = 2$ $\mu A/cm^2/msec^{1/2}$ and three different values of ρ_0. $\rho_0 = 0$ (*pluses*), $\rho_0 = 1500$ Hz (*crosses*), and $\rho_0 = 3000$ Hz (*stars*). The *solid line* corresponds to $R = 0.22(\rho/1000)^3$. The average firing rate was computed over 300 sec.

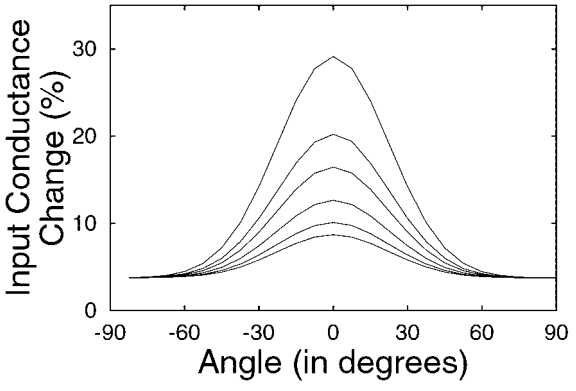

Figure 7. The tuning curves of the input conductance are contrast invariant. The change in input conductance of the neurons is shown against the orientation of the stimulus for different values of the contrast. From *top* to *bottom* in Hz: $\rho_1 = 10000, 6500, 5000, 3500, 2500, 1950$. The width of the stimulus dependent input is $\Delta = 22.5°$. For all these curves $\rho_0 = 1500$ Hz.

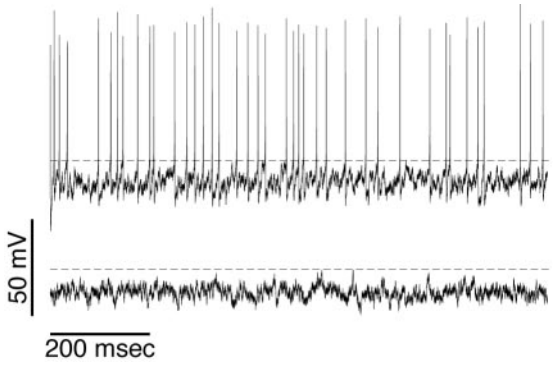

Figure 8. The neuronal discharge is noise driven as seen on the traces of membrane potential. *Top*, The stimulus is at optimal orientation. *Bottom*, The stimulus is at null orientation. The *dashed line* is the level of depolarization at the rheobase ($V_c = -57.6$ mV). $\rho_0 = 1500$ Hz; $\rho_1 = 5000$ Hz; $\Delta = 22.5°$. In both the preferred and null orientation the mean voltage is below rheobase.

different contrast levels. As the contrast increases, the input conductance increases at the preferred orientation by up to 50% of its value at rest. However, at null orientation it remains almost independent of the contrast. Moreover, the width of the tuning curve relative to the baseline is contrast independent and is equal to Δ.

The traces of the membrane potential of the model neuron in response to a visual stimulus is plotted in Figure 8 at the preferred and null orientations for two values of the contrast. On average, membrane potentials are significantly below the firing threshold of the neurons, yet the neuron can fire action potentials. For instance, at preferred orientation the neuron fires with an average firing rate of 30 Hz. This substantial level of activity is a consequence of the large fluctuations of the neuron potential that are induced by the noise. The tuning curve of the SD of these fluctuations is plotted in Figure 9*A* for different contrasts. It shows that for the chosen model parameters the fluctuation level is similar to the one observed in the experiments of Anderson et al. (2000a,b). It also demonstrates that as in these experiments, the fluctuations are weakly tuned and contrast independent. Note however that these fluctuations were computed after cutting the action potentials (i.e., by clipping the potential below the threshold V_c). A much more pronounced tuning of the fluctuations is found if the action potentials are not suppressed (data not shown).

Figure 9, *B* and *C*, displays the tuning curves of the average membrane potentials and the average firing rates of the neuron, respectively, for different input levels. The *solid lines* in Figure 9 correspond to the best Gaussian fit of the simulation results. These results show that both tuning curves are approximately contrast invariant in most of the range of contrast studied; see *insets.* Figure 9*D* displays the width of the spike response against the firing rate at preferred orientation. Visual inspection shows that the tuning of the spike response is sharper than the input tuning. The sharpening factor is ~1.7, in agreement with the exponent of the approximate power law presented in Figure 6*B* for $\rho_0 = 1500$ Hz, $\alpha = 3$. This is similar to the results obtained analytically for the simplified rate and integrate-and-fire model. It shows that despite all the nonlinearities acting on a large spectrum of time scales that are present in the dynamics of our conductance-based model, noise is still able to induce contrast invariance of the output spiking rate as well as the average membrane potential. This also implies that as in the integrate-and-fire model, the rate and the average membrane potential can be related by a power law. This is confirmed in Figure 10. Note that the exponent, γ, of this power law is slightly larger than the exponent α. Therefore the tuning of the membrane potential should be slightly broader than the tuning of the input. This is confirmed by a detailed analysis of our simulation results (data not shown).

DISCUSSION

The mechanism for contrast invariance of the output firing rate

It has been reported that noise in the input can contribute to contrast invariance (Anderson et al. 2000a; M. Shelley and D. McLaughlin, unpublished observations). Up to now the mechanism governing this occurrence was not fully understood. Our

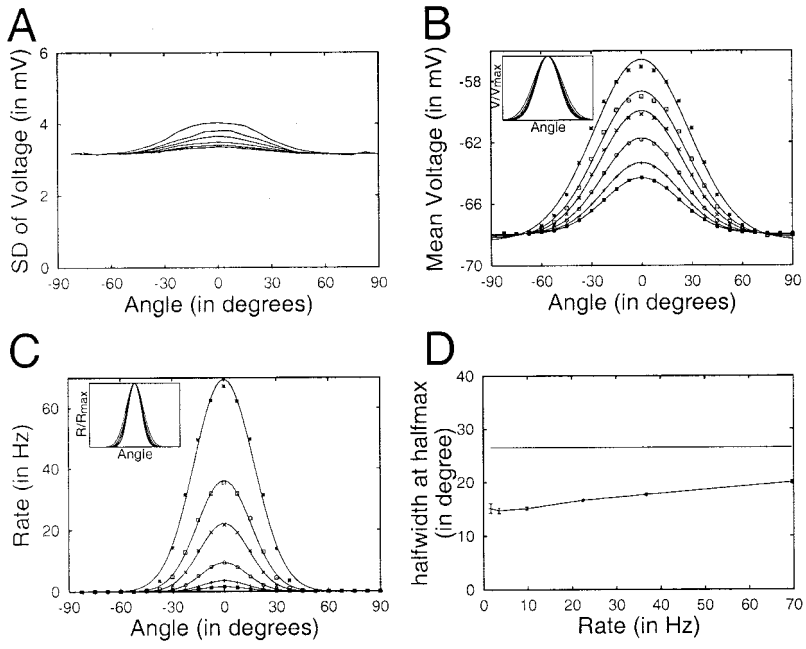

Figure 9. Tuning curves for different contrasts. Parameters are as in Figure 7 (contrast decreases from *top* to *bottom*). Results are averaged over 30 sec of simulation. *A*, The SD of the membrane potential fluctuations depends only weakly on the stimulus orientation. The SD was calculated after clipping the spikes at $V = V_c = -57.6$ mV. The tuning of the average membrane potential (*B*) and the spike response R (*C*) are approximately contrast invariant in most of the contrast range studied. *B*, *Inset*, After normalization to the average membrane potential at the preferred orientation the tuning curves of the average membrane potential are superimposed. *C*, *Inset*, Spike responses after normalization to the response at optimal orientation. *D*, The tuning of the output rate is sharper than the tuning of the input. The width of the output rate and average voltage are plotted against the rate at the preferred orientation. The width was estimated by fitting the simulation results with a Gaussian (see Materials and Methods). The error bars are for the error estimate of the fit. The *horizontal line* corresponds to the half-width at half-maximal of the input (26.5°).

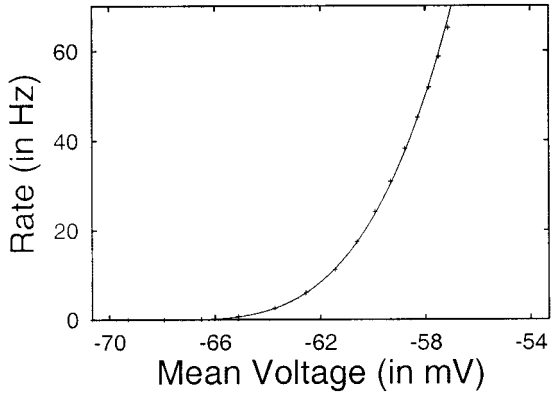

Figure 10. The output rate and the average membrane potential can be related by a power law. The average rate and the average membrane potential were computed in simulations for $\sigma = 2\ \mu A/cm^2/msec^{1/2}$. The *continuous line* was obtained by fitting the simulations results with $R = A(\bar{V} - V^*)^{\gamma}$. Here V^* is the value of the average voltage at cross-orientation in Figure 9*B*: $V^* = -68.05$ mV. The fit parameters are $A = 0.015 \pm 10^{-3}$, $\gamma = 3.51 \pm 0.04$.

analysis clarifies the mechanism for contrast invariance of the output, provided that the input is contrast invariant. We have seen that contrast invariance is exact if the effective transfer function of the neuron is a power law. Although in general this is not the case, we have shown that the interplay between noise and threshold nonlinearity leads to an approximate contrast invariance of the output for a certain range of the stimulus contrast, provided that the noise is chosen appropriately. In this scheme the threshold of the effective transfer function of the neuron is very close to zero. The effect of the noise is to transmute the threshold nonlinearity of the noiseless neuron into a power law without a threshold. This mechanism is different from linearization by noise that has been studied extensively.

We have shown that this mechanism is a general one. In the integrate-and-fire that we have studied, we found that the firing rate of the neuron can be related to its input with a very good approximation by a power law. The average voltage, $\bar{V}$, varies linearly with the input because $\bar{V}$ remains subthreshold where the neuron behaves like a passive integrator. Deviations from this linear behavior, attributable to the resetting at threshold, occur only when the rate becomes too large. Combining these two properties shows that $\bar{R}$ and $\bar{V}$ are related as $\bar{R} \propto \bar{V}^{\alpha}$ for some $\alpha > 0$. This is similar to our result for the threshold linear rate model. Our analysis of the conductance-based model leads to similar conclusions. The main difference with the integrate-and-fire model is that because of active processes, the deviations from linearity in the relationship between the input and the average potential are more pronounced. However, the relationship between the average potential and the input can still be related by an approximate power law. The exponent of this power law, γ, remains close to the exponent, α, of the power law relating the firing rate to the input.

The limitations

In the absence of input the firing rate of the neuron should be very small. Thus the noise level, σ (which is contrast independent), cannot be too large. On the other hand the exponent α, which determines the degree of sharpening of the spike rate tuning, is a decreasing function of σ. This imposes an upper limit on the noise level.

These constraints on σ limit the range of contrast over which the output rate tuning is contrast invariant. This was shown analytically for the rate and the integrate-and-fire models and confirmed numerically with simulations for a conductance-based model. This limitation on the contrast puts an upper bound on the maximum firing rate for which the mechanism holds. In our simulations of the conductance-based model using realistic parameters, the contrast invariance of the spike response breaks down when the firing rate of the neuron is >30 Hz.

The input to the cells

In the spiking models we assumed that the average input to the neuron is contrast invariant and that the input fluctuations are independent of contrast. Under these conditions, the tuning of both the firing rate and the average potential are contrast invari-

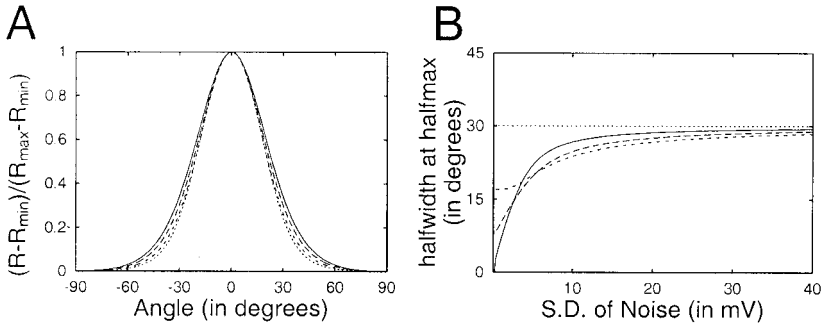

Figure 11. *A*, Normalized tuning curves of the spike rate elevation, using the same parameters as in Figure 2*C*. In Figure 2*C* the contrast independence breaks down because the rate at the null orientation is not negligible. Subtracting the minimum rate overcomes this, resulting in contrast invariance of the rate elevation tuning. *B*, Half-width at half-maximal for the rate elevation, using the same parameters as in Figure 3. The half-width at half-maximal of the rate becomes nondefined for large noise levels, because of the high rate at the null orientation. This does not create a problem for the firing rate elevation. The effect of increasing the noise is to increase the half-width at half-maximal of the response to that of the input at the highest noise levels. This extreme describes the classical threshold linearization attributable to noise. The result is that the tuning curves of the firing rate elevation are contrast invariant for all noise levels above 3 mV. In both *A* and *B* rate elevation was determined by subtracting the rate at cross-orientation.

ant, in line with experimental results (Anderson et al., 2000a). As in these experimental findings, this also lead to contrast-independent voltage fluctuations. Our analysis shows that conversely the contrast invariance of the voltage and rate tuning, combined with the contrast independence of the voltage fluctuations, can be achieved only if the average input tuning is contrast invariant and the input noise is contrast independent.

The contrast invariance of the average input tuning can be explained by a purely feedforward mechanism of orientation selectivity. Indeed, in this mechanism complex cells receive their input from simple cells, the output of which is contrast invariant. However, as we have seen, invariance will occur only in a rather limited range of inputs. Recurrent interactions could extend this range through effective gain control. Alternatively, they could extend the range of the output for which the tuning is contrast invariant by sharpening the input at high contrast, thus offsetting the broadening of the tuning curve that would occur otherwise.

Explaining the contrast independence of the input fluctuations is more difficult. If this noise is caused by the irregular activity of the simple cells, it should increase with contrast. Fluctuations in the recurrent feedback in the local network would also be contrast dependent. Thus where do the stimulus independent fluctuations originate? This remains unresolved.

Experimental issues

Two different definitions of contrast invariance have been used in the literature. One is the contrast invariance of the firing rate tuning and the other is the contrast invariance of the tuning of the firing rate elevation. The latter is less restrictive because it does not require a small baseline activity compared with the evoked one. If one uses this definition, contrast invariance can be obtained even if the noise level is high. This is shown in Figure 11*A* for $\sigma = 8$ mV. These tuning curves are nearly perfectly contrast invariant, unlike the tuning curves shown in Figure 2*C*. However, the width of the tuning curves is now significantly broader than for $\sigma = 4$ mV (Fig. 2*B*). This width is almost the same as the width of the voltage tuning. This is because for high noise level there is no sharpening of the input because the effective gain function of the neuron is close to linear. The width of the tuning curve of the firing rate elevation is plotted against the noise level in Figure 11*B* for three different contrast levels. This shows that for σ above 4 mV the three curves coincide. However, if σ increases further, the width approaches the width of the potential tuning. Therefore the different definitions of contrast invariance can lead to qualitatively different conclusions.

Independently of the model we have found that the mean firing rate is related to the average voltage by a power law. This prediction is general because it is a consequence of the biophysics of the neurons. It could be tested by intracellular experiments *in vivo* for neurons in V1 as well as in other areas. As long as the noise is stimulus independent and the average membrane potential is sufficiently subthreshold, this property should be observed unless active currents significantly affect the subthreshold neuron dynamics.

A further experimental test of the mechanism proposed here would be to measure the neuronal response when noise is injected into the neuron. Our theory predicts that adding extra noise to the neuron should increase the firing rate and broaden the spike tuning curve, and the tuning of the rate elevation should continue to be contrast invariant.

For neurons in V1 the exponent of the power is directly related to the amount of sharpening. This can also be tested experimentally. It should be noted that power law compressive nonlinear transfer functions have also been suggested to account for the way neurons in the Macaque primary visual cortex respond to gratings and plaids (Carandini et al., 1997) in the framework of the "normalization model" proposed by Heeger (1991, 1992). In this study a power law with an exponent around 2 was found to account for the data recorded extracellularly. In our study of the conductance-based neuron model, we find an exponent of 3.9, significantly larger than that reported by Heeger (1991, 1992). It is unclear whether this difference reflects a misrepresentation of the input noise in our model or whether the model parameters of our V1 neuron deviate substantially from those of the complex cells in V1.

Deviations from the power law relationship between average firing rate and average voltage are expected to occur if the firing rate is too high. For high contrast, the invariance to contrast of the output tuning should start to break down near the preferred orientation but will still hold sufficiently far from it. Therefore, the spike rate tuning width derived from fitting the output tuning curve with a Gaussian is not sensitive to these deviations. However, one can fit the output with the function $f(\theta) = a(1 + b \exp(-c\theta^2 - d\theta^4))$, which is more sensitive to these deviations.

In conclusion, we have shown that noise can play a role in achieving contrast invariance of orientation tuning in V1. However, this mechanism is strongly constrained by a tradeoff between the sharpening of the response and the range in contrast that can be accommodated. The results presented here indicate that noise can account for contrast invariance of spike outputs that are sharper than the input by a factor in the range of 1–2 and for firing rates that are below 30 spikes per second. Whether these numbers are typical for neurons in V1 requires further exploration.

Note added in proof. After this work was completed we became

aware that some of the results derived here regarding the behavior of the rate model have also been obtained independently by K. Miller and T. Troyer (2002). We thank them for informing us about their work.

APPENDIX A: The effective transfer function for the threshold linear rate model with Gaussian noise

Here we derive the effective transfer function, G_σ, for a threshold linear neuron with Gaussian noise of width σ in the voltage. The effective transfer function is given by:

$$G_\sigma(\bar{V}) \equiv \langle G(\bar{V} + \sigma\eta)\rangle_\eta = \int_{-\infty}^{\infty} G(\bar{V} + \sigma\eta)P(\eta)d\eta, \quad (24)$$

where $P(\eta)$ is the probability distribution of the noise.

For a threshold linear neuron with Gaussian noise, G is given by $G(V) = \beta[V - V_T]_+$, and P satisfies $P(\eta) = \exp(-\eta^2/2)/\sqrt{2\pi}$. Thus:

$$\begin{aligned} G_\sigma(\bar{V}) &= \int_{-\infty}^{\infty} \beta[\bar{V} - V_T + \sigma\eta] + \frac{e^{-\eta^2/2}}{\sqrt{2\pi}}d\eta \\ &= \beta\int_{-(\bar{V}-V_T)/\sigma}^{\infty} (\bar{V} - V_T + \sigma\eta)\frac{e^{-\eta^2/2}}{\sqrt{2\pi}}d\eta \\ &= \beta(\bar{V}-V_T)\int_{-(\bar{V}-V_T)/\sigma}^{\infty} \frac{e^{-\eta^2/2}}{\sqrt{2\pi}}d\eta + \beta\sigma\int_{-(\bar{V}-V_T)/\sigma}^{\infty} \frac{\eta e^{-\eta^2/2}}{\sqrt{2\pi}}d\eta \\ &= \beta\sigma\left\{\frac{\bar{V} - V_T}{\sigma}H\left(\frac{\bar{V} - V_T}{\sigma}\right) + \frac{\exp(-(\bar{V} - V_T)^2/2\sigma^2)}{\sqrt{2\pi}}\right\}, \end{aligned} \quad (25)$$

where H is the complementary error function, $H(x) = \int_x^\infty e^{-y^2}/2\, dy/\sqrt{2\pi}$.

APPENDIX B: The effective transfer function, average voltage, and voltage fluctuations for the integrate-and-fire neuron

Here we calculate the mean firing rate, average voltage, and SD of the voltage fluctuations for an integrate-and-fire neuron that receives stochastic Gaussian input. From the stochastic Equation 3, a Fokker–Planck equation for the probability density function $\rho(V, t)$ of the voltage can be derived (Gluss, 1967; Tuckwell, 1984).

The probability density function ρ satisfies:

$$\frac{\partial}{\partial t}\rho(V, t) = -\frac{\partial}{\partial V}J(V, t) + \delta(V - V_{reset})J(V_T, t), \quad (26)$$

where $J(V, t)$ is the flux through voltage V at time t, given by:

$$J(V, t) = \left(\frac{g_L}{C_M}(V_{rest} - V) + \frac{1}{C_M}I - \frac{\sigma^2}{2C^2}\frac{\partial}{\partial V}\right)\rho(V, t), \quad (27)$$

and the term $\delta(V - V_{reset})J(V_T, t)$, where $\delta(.)$ is the Dirac δ-function (Dirac, 1924), describes the reset when the neuron reaches threshold.

After sufficient time has passed, the voltage distribution will have evolved to the equilibrium distribution, $\rho(V, t) \to \rho_{eq}(V)$, which is given by (Gluss, 1967; Tuckwell, 1984):

$$\rho_{eq}(V) = A\exp[-B(V_0 - V)^2]\int_{V_{reset}}^{V_T}\exp[B(V_0 - V')^2]dV', \quad (28)$$

for $V < V_{reset}$, and:

$$\rho_{eq}(V) = A\exp[-B(V_0 - V)^2]\int_{V}^{V_T}\exp[B(V_0 - V')^2]dV', \quad (29)$$

for $V_{reset} < V < V_T$. Here $B = g_L C_M/\sigma^2$ and $V_0 = V_{rest} + I/g_L$. The validity of this solution can be checked by inserting it into Equations 26 and 27. For the flux J_{eq} this yields $J_{eq}(V) = 0$ for $V < V_{reset}$ and $J_{eq}(V) = \sigma^2 A/2C_M^2$ for $V_{reset} < V < V_T$. As a result $\partial\rho_{eq}(V)/\partial t = 0$, as it should be for the equilibrium distribution.

The constant A is determined by the normalization of ρ_{eq}, $\int \rho_{eq}(V)dV = 1$, and satisfies:

$$A = \frac{2B}{\sqrt{2\pi}}\left[\int_{x_-}^{x_+} e^{x^2/2}H(x)dx\right]^{-1}, \quad (30)$$

where $x_- = \sqrt{2B}(V_0 - V_T)$, and $x_+ = \sqrt{2B}(V_0 - V_{reset})$.

The mean firing rate $\bar{R}$ is given by the flux through the threshold voltage, $J_{eq}(V_T)$:

$$\bar{R} = \frac{\sigma^2}{2C_M^2}A = \frac{g_L}{C_L}\left[\sqrt{2\pi}\int_{x_-}^{x_+} e^{x^2/2}H(x)dx\right]^{-1}. \quad (31)$$

The mean voltage $\bar{V}$ can also be calculated using the equilibrium distribution of the voltage. Using $\bar{V} = \int_{-\infty}^{V_T} V\,\rho_{eq}(V)dV$ one obtains, after some manipulation:

$$\bar{V} = V_{rest} + g_L^{-1}I - (V_T - V_{reset})\tau_M\bar{R}. \quad (32)$$

Likewise, the SD of the subthreshold voltage, σ_V, can be computed from $\sigma_V^2 = \int_{-\infty}^{V_T}(V - \bar{V})^2\rho_{eq}(V)dV$ and is given by:

$$\sigma_V^2 = \frac{\tau_M}{2}\left(\frac{\sigma}{C}\right)^2 + (V_T - V_{reset})\left(\bar{V} - \frac{V_T + V_{reset}}{2}\right)\tau_M\bar{R}. \quad (33)$$

REFERENCES

Anderson JS, Lampl I, Gillespie DC, Ferster D (2000a) The contribution of noise to contrast invariance of orientation tuning in cat visual cortex. Science 290:1968–1972.

Anderson JS, Carandini M, Ferster D (2000b) Orientation tuning of input conductance, excitation, and inhibition in cat primary visual cortex. J Neurophysiol 84:909–926.

Arieli A, Sterkin A, Grinvald A, Aertsen A (1996) Dynamics of ongoing activity: explanation of the large variability in evoked cortical responses. Science 273:1868–1871.

Ben-Yishai R, Lev Bar-Or R, Sompolinsky H (1995) Theory of orientation tuning in visual cortex. Proc Natl Acad Sci USA 92:3844–3848.

Ben-Yishai R, Hansel D, Sompolinsky H (1997) Traveling waves and processing of weakly tuned inputs in cortical module. J Comp Neurosci 4:57–77.

Bernander O, Douglas RJ, Martin KA, Koch C (1991) Synaptic background activity influences spatiotemporal integration in single pyramidal cells. Proc Natl Acad Sci USA 88:11569–11573.

Borg-Graham LJ, Monier C, Fregnac Y (1998) Visual input evokes transient and strong shunting inhibition in visual cortical neurons. Nature 393:369–373.

Brunel N, Chance FS, Fourcaud N, Abbott LF (2001) Effects of synaptic noise and filtering on the frequency response of spiking neurons. Phys Rev Lett 86:2186–2189, 2001.
Carandini M, Heeger DJ, Movshon JA (1997) Linearity and normalization in simple cells of the macaque primary visual cortex. J Neurosci 17:8621–8644.
Dirac PAM (1995) The collected works of P.A.M. Dirac, 1924–1948 (Dalitz RH, ed). Cambridge, UK: Cambridge UP.
Ermentrout GB (1994) Reduction of conductance based models with slow synapses to neural nets. Neural Comput 6:679–695.
Ferster D, Miller KD (2000) Neural mechanisms of orientation selectivity in the visual cortex. Ann Rev Neurosci 23:441–471.
Gerstner W (2000) Population dynamics of spiking neurons: fast transients, asynchronous states, and locking. Neural Comput 12:43–89.
Gluss B (1967) A model for neuronal firing with exponential decay of potential resulting in diffusion equations for the probability density. Bull Math Biophys 29:233–243.
Hansel D, Sompolinsky H (1998) Modeling feature selectivity in local cortical circuits. In: Methods in neuronal modeling (Koch C, Segev I, eds), pp 499–569. Cambridge, MA: MIT.
Heeger DJ (1991) Nonlinear model of neural responses in cat visual cortex. In: Computational models of visual processing (Landy M, Movshon JA, eds), pp 119–133. Cambridge, MA: MIT.
Heeger DJ (1992) Normalization of cell responses in cat striate cortex. Vis Neurosci 9:181–198.
Hubel DH, Wiesel TN (1962) Receptive fields, binocular interaction and functional architecture of the cat's visual cortex. J Physiol (Lond) 160:106–154.
Li C, Creutzfeld O (1984) The representation of contrast and other stimulus parameters by single neurons in area 17 of the cat. Pflügers Arch 401:304–314.
Miller TD, Troyer TW (2002) Neural noise can explain expansive, power-law nonlinearities in neural response functions. J Neurophysiol 87:653–659.
Rapp M, Yarom Y, Segev I (1992) The impact of parallel fiber background activity on the cable properties of cerebellar Purkinje cells. Neural Comput 4:518–532.
Sclar G, Freeman RD (1982) Orientation selectivity in the cat's striate cortex is invariant with stimulus contrast. Exp Brain Res 46:457–461.
Shriki O, Hansel D, Sompolinsky H (1998) Modeling neuronal networks in cortex by rate models using the current–frequency response properties of cortical cells. Soc Neurosci Abstr 24:143.
Skottun BC, Bradley A, Sclar G, Ohzawa I, Freeman RD (1987) The effects of contrast on visual orientation and spatial frequency discrimination: a comparison of single cells and behavior. J Neurophysiol 57:773–786.
Somers D, Nelson S, Sur M (1995) An emergent model of orientation selectivity in cat visual cortical simple cells. J Neurosci 15:5448–5465.
Sompolinsky H, Shapley R (1997) New perspectives on the mechanisms for orientation selectivity. Curr Opin Neurobiol 7:514–522.
Troyer TW, Krukowski AE, Priebe NJ, Miller KD (1998) Contrast-invariant orientation tuning in cat visual cortex: thalamocortical input tuning and correlation-based intracortical connectivity. J Neurosci 18:5908–5927.
Tsodyks MV, Kenet T, Grinvald A, Arieli A (1999) Linking spontaneous activity of single cortical neurons and the underlying functional architecture. Science 286:1943–1946.
Tuckwell HC (1984) Introduction to theoretical neurobiology. Cambridge, UK: Cambridge UP.